# BASIN SCALE CONCEPT VALIDATION: Urban Hydrology Model
## Draft 09/13/12

By: Olivia Wright and Erkan Istanbulluoglu

## Effective Impervious Area

A rainfall-runoff depth analysis of storm events is used to estimate the effective impervious area of the basin and the initial abstraction of impervious surfaces (*Boyd et al.* 1993, 1994). The analysis evaluates the runoff depth of each storm as a function of the storm's precipitation depth. The slope of the relationship estimates the fraction of the basin that contributes to runoff, and the rainfall axis intercept estimates the initial abstraction that must be satisfied before runoff can occur.

Storm events were calculated by summing consecutively occurring hourly precipitation. Individual storm events were separated by 24 hours of no precipitation. Due to the responsiveness of our basin, we assumed the runoff event occurred during the same time period as the precipitation event. Plotting the full range of observed storm events estimates an initial abstraction as 4 mm. Runoff can be calculated as:

$$R = (P - I_a) * C * EIA$$

$P$ is precipitation (hourly)
$I_a$ is initial abstraction
$C$ is runoff coefficient
$EIA$ effective impervious fraction in basin

Figure 1 shows the rainfall-runoff depth plot for dry season storm events with initial abstraction removed. The analysis focused on surface runoff with baseflow removed. The effective impervious area during dry season storm events ranged from approximately 9-20%. For summer rainfall, we assume that effective impervious area (EIA) is the dominant source of runoff and the slope that captures the high end of storm event depths can be assumed to be EIA.

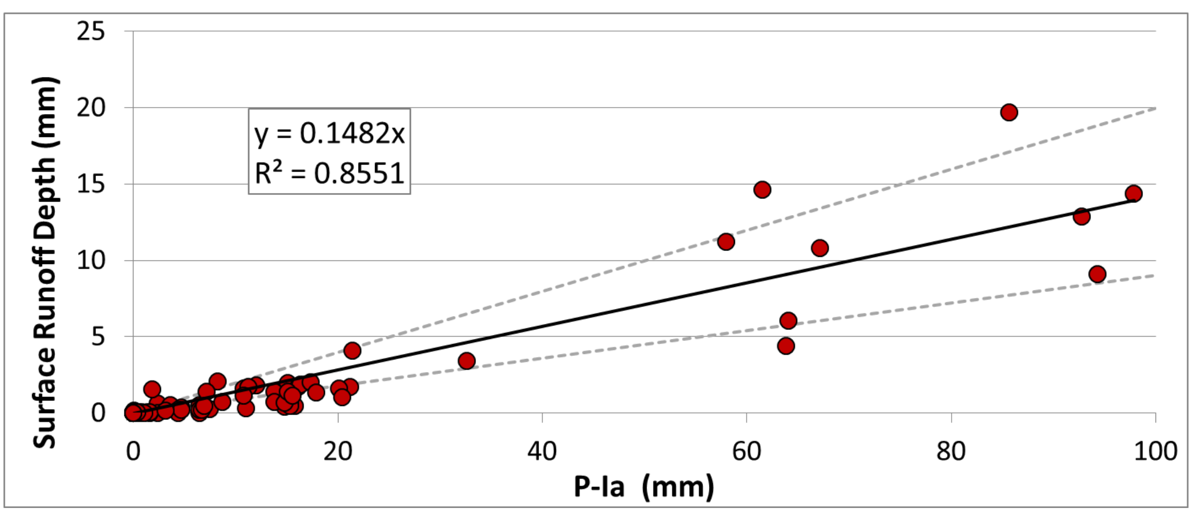


Figure 1. Rainfall- runoff depth plots

Table 1 presents the area of the impervious land use categories and the fraction of the basin they cover. The total impervious area (TIA) calculated from spatial data is 70% of the basin, while the estimated EIA is 20%.

| Impervious Category | Area (acres) | Fraction of Basin |
|---|---|---|
| Roads | 41.32 | 0.15 |
| Rooftop | 24.92 | 0.09 |
| Other | 120.10 | 0.45 |
| **Total Impervious Area** | **186.34** | **0.70** |
| **Effective Impervious Area** | **53.46** | **0.20** |

Table 1. Impervious land cover area and fraction of basin

## Hydrologic Modeling of land processes and LID treatment

This study uses a lumped Urban Hydrology Model to estimate the long term hydrologic behavior of Newaukum Urban basin considering current land cover [Istanbulluoglu et al., 2012], figure 2. The model is a lumped representation of an urbanized landscape.

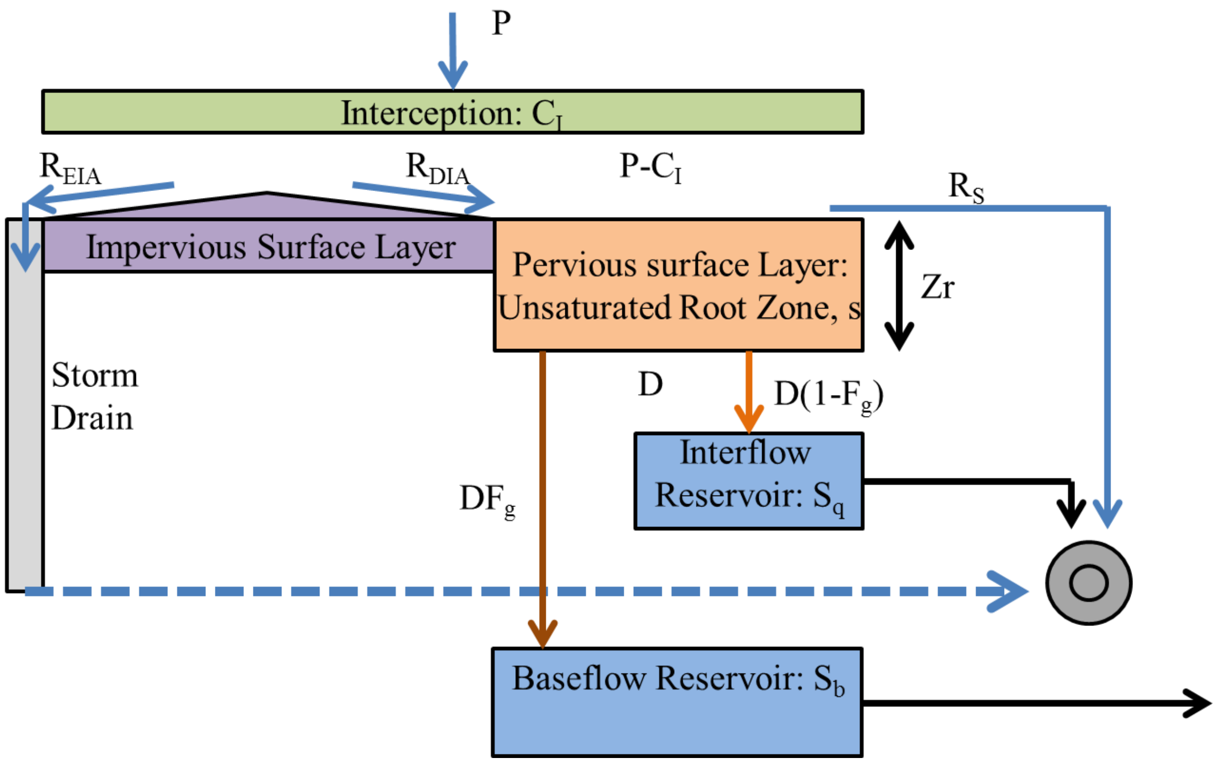


Figure 2. Conceptual representation of the processes in the Urban Hydrology Model

The depth averaged soil moisture in the root zone layer is calculated by the mass balance equation (*Istanbulluoglu*, 2012)

$$nZ_r \frac{ds}{dt} = I_a - ET_a(s) - D(s)$$

$n$ is porosity

$Z_r$ is effective rooting depth

$s$ is soil moisture
$t$ is time
$I_a$ is infiltration rate
$ET_a$ is actual evapotranspiration rate
$D$ is drainage

Interception from the canopy is calculated by:

$$C_I = \min(I_{\max} V_t, PV_t)$$

$I_{max}$ is a maximum hourly interception
$V_t$ is the fraction of vegetation cover on the land surface (includes dry and live biomass)
$P$ is depth of rainfall

When $P$ is larger than $C_I$, throughfall occurs at the same rate as precipitation. The precipitation duration reaching the ground is reduced to account for initial filling of the canopy storage during the early part of the rain event. When the soil is unsaturated, the infiltration rate is determined by the minimum of the precipitation rate and the infiltration capacity. After soil saturation, the infiltration rate is reduced to the drainage rate:

$$I_a = \begin{cases} \min[p, I_c] & 0 \le s < 1 \quad P > C_I \\ D & s = 1 \quad P > C_I \end{cases}$$

$I_c$ is infiltration capacity
$p$ is average pervious input rate

$$p = (P - C_I) + \frac{((P - C_I) * (IMPfrac - EIAfrac) * Coeff)}{1 - IMPfrac}$$

*IMPfrac* is the impervious surface fraction of the basin
*EIAfrac* is the effective impervious fraction of the basin
*Coeff* is the runoff coefficient

Surface runoff occurs when $p$ exceeds $I_a$ and is approximated by:

$$R_s = \begin{cases} (p - I_a) & p > I_a \\ 0 & p \le I_a \end{cases}$$

The root zone layer is assumed to have uniform soil texture, porosity, and hydraulic conductivity. The drainage of the soil column by gravity is modeled to occur at the lowest boundary of the soil layer. At soil saturation, the drainage is at its maximum and is calculated as the saturated hydraulic conductivity ($K_s$) and decays exponentially to a value of zero at field capacity, $s_{fc}$.

$$D(s)=\begin{cases} Ks & s=1 \\ K(s)=K_s s^{2b+3} & s_{fc}<s\le 1 \end{cases}$$

*K(s)* is unsaturated hydraulic conductivity
*b* is an empirical parameter in the Campbell soil moisture retention model (*Campbell*, 1974)

Actual evapotranspiration is calculated using a soil moisture limitation approach (*Laio et al.*, 2001; *Istanbulluoglu et al.*, 2011):

$$ET_a = PET \cdot \beta_s(s)$$

*PET* is the potential evapotranspiration
$\beta_s$ is evapotranspiration efficiency term based on soil moisture

$$\beta_s(s)=\begin{cases} 0, & s_h < s \le s_w \\ \dfrac{s-s_w}{s^*-s_w}, & s_w < s \le s^* \\ 1 & s_* < s \end{cases}$$

$s_h$ is soil hygroscopic capacity
$s_w$ is soil moisture at wilting point
$s^*$ is soil moisture at stomata closure

Hourly potential evapotranspiration is calculated using the Priestly Taylor method:

$$PET=\alpha\frac{\Delta}{\Delta+\gamma}\frac{(R_N-G)}{\rho_w\lambda_v}$$

$\Delta$: slope of the saturation vapor pressure – temperature relationship (kPa $^oC^{-1}$);
$R_N$: net radiation at the evaporating surface (W/m$^2$)
G: ground heat flux (W/m$^2$);
$\lambda_v\rho_w$: latent heat of vaporization (28.34 Wd m$^{-2}$ mm$^{-1}$) or (680.16 Wh m$^{-2}$ mm$^{-1}$ for hourly);
$\gamma$ : is the psychronometric constant (kPa $^oC^{-1}$)
$\alpha = 1.26$

Baseflow is calculated as:

$$R_b=\frac{1}{T}S$$

*S* is the reservoir storage
*T* is the reservoir drainage time scale

Runoff from the effective impervious are must be distinguished from p and Rs because EIA is directly connect to the storm drain. Runoff from effective impervious areas is calculated as:

$$R_{EIA}=(P-C_I)*EIAfrac*Coeff$$

Total streamflow from the basin is calculated as:

$$R = R_b + R_s + R_{EIA}$$

The model also includes a dynamic vegetation component that updates the amount of biomass and LAI below and above ground [Istanbulluoglu et al., 2012].

## Model Variations and Decision variables

Three variations of the model are evaluated to determine the effectiveness of BMP application: (1) Urban land use (no BMPs), (2) Urban land use with BMP treatment and (3) forested conditions.

The urban land use model with no BMP treatment simulates existing hydrologic conditions to evaluate the current health of the catchment. The urban land use with BMP treatment model simulates the impact various BMP treatment scenarios have on basin hydrology. The forested model simulates the hydrology of the basin with a natural landscape prior to development. The forested condition is used to further evaluate the effectiveness of the BMP scenario model.

## Model input and calibration

The model is forced with precipitation and potential evapotranspiration. Input to the model includes the basin's total impervious fraction, effective impervious fraction, and runoff coefficient.

| | |
|---|---|
| **Total Impervious Fraction** | **0.70** |
| **Effective Impervious Fraction** | **0.20** |
| **Coefficient** | **0.90** |

Table 2. Model basin characteristic input values

The urban land use (no BMPs) modele is calibrated to 3 years of observed streamflow data. The calibration parameters of the model are *Fg*, *Variable Infiltration Capacity (VIC) b-shape parameter*, and *T*. *Fg* controls the fraction of drainage water that directly contributes to groundwater, *VIC b-shape parameter* controls the shape of the infiltration capacity curve, and the *T* controls the reservoir drainage timescale. Model calibration was performed using flow duration curves and the Nash-Sutcliffe (NS) model efficiency coefficient to match the modeled runoff to observed. Figures 3(a-c) are calibration plots for the first year of observed data. Figures 4(a-c) are calibration plots for the 3 years of observed data.

***High flow 1-year Model Calibration***

- First year of observed data
- Calibration parameters: Fg=0.79, VIC b-shape =1, Tdecay=4
- Modeled and observed streamflow difference: 2.60 mm
- NS: 0.72

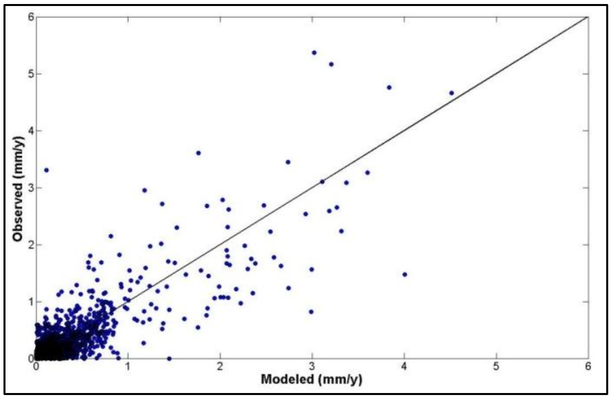


Figure 3a. Modeled vs observed streamflow

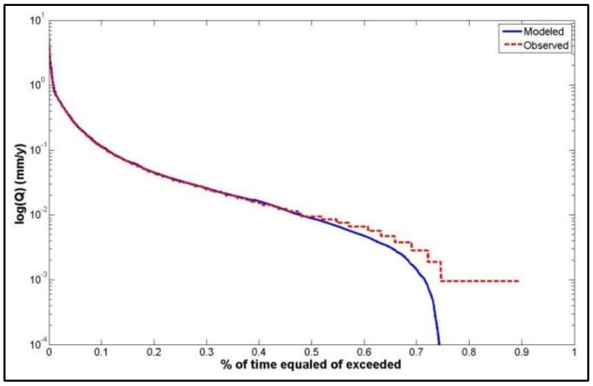


Figure 3b. Flow duration curve

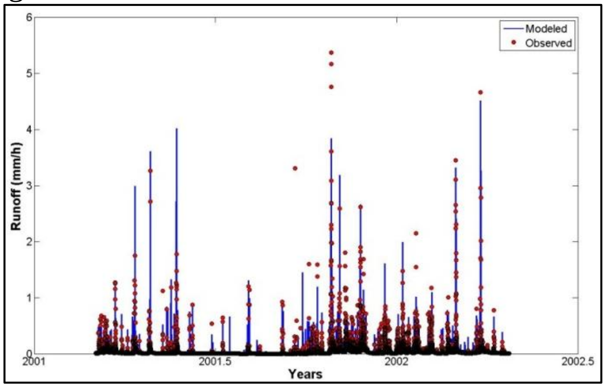


Figure 3c. Observed and modeled streamflow

***3 year calibration:***

- 3 years of observed streamflow
- Calibration parameters: Fg=0.87, VIC b-shape =0.1, Tdecay=18
- Modeled and observed streamflow difference: 11.35 mm
- NS: 0.52

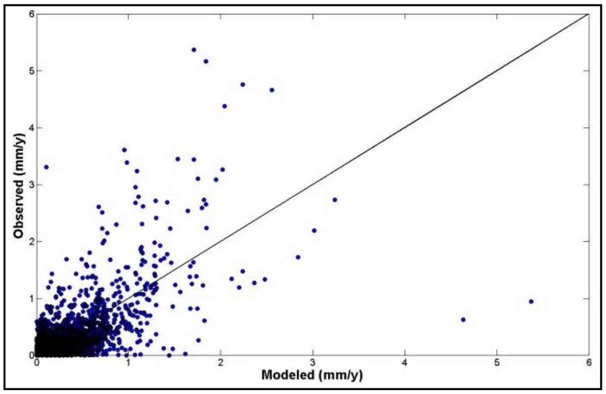


Figure 4a. Modeled vs observed streamflow

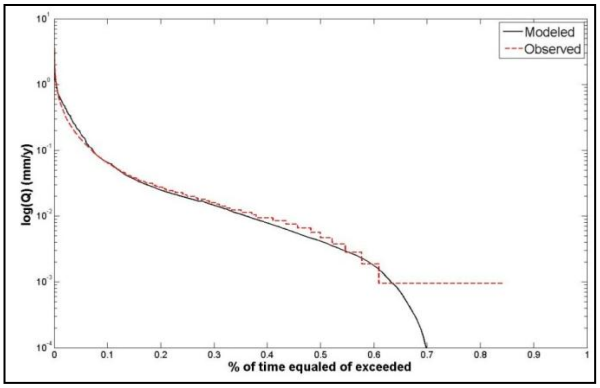


Figure 4b. Flow duration curve

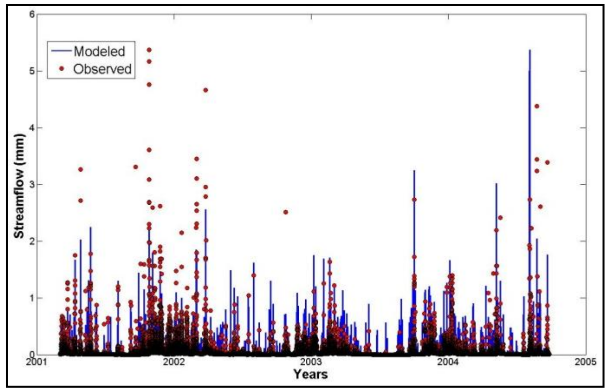


Figure 4c. Observed and modeled streamflow

Using the modeled 3 year calibration parameters, Newaukum Urban runoff was generated for 12 years using observed precipitation forcing data.

***Water Balance Output***

During model calibration, we found a significant portion of drainage water contributing to groundwater storage, with an estimated Fg value of 0.87. Furthermore, the groundwater storage seems to be lost from the basin (Figure 5). Due to the location of the catchment at the headwaters of Newaukum Creek basin, our model calibration assumes groundwater storage bypasses the Newaukum Urban outlet and joins the channel network farther downstream in the basin.

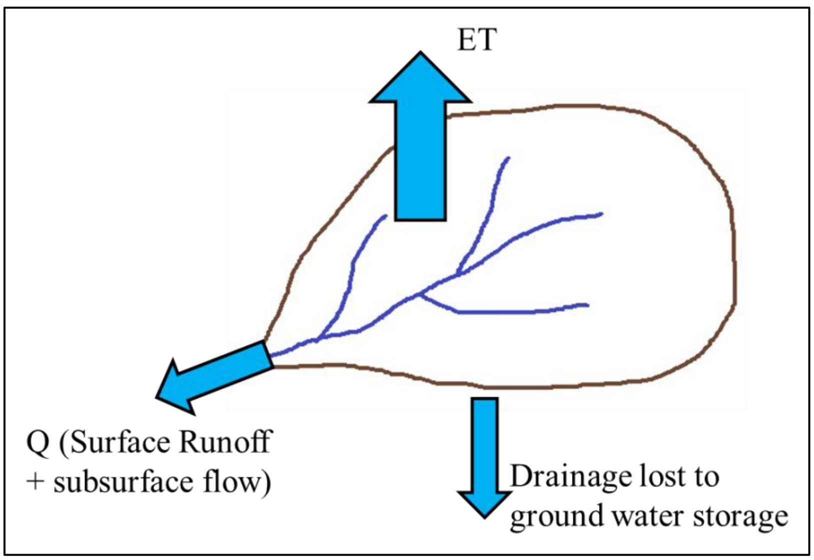


Figure 5. Catchment water balance

To verify the accuracy of our model, we calculated the water balance ratios to ensure water balance closure. Table 3 presents the ratios for the 3-year calibration period.

| Model Output | ETa/P | Q/P | Drainage/P |
|---|---|---|---|
| 3 year calibration Urban | 0.321 | 0.240 | 0.466 |

Table 3. Water basin ratios for Urban, 3-year calibration

**Bioretention Model: Bucket Grassland Model (BGM)**
Bioretention cells are modeled using a modified lumped bucket hydrology model, the Bucket Grassland Model (BGM) (*Istanbulluoglu et al.*, 2012), Figure 7. Our modifications include a ponding layer above the soil layer. The ponding layer captures the surface runoff until the ponding volume exceeds the storage volume, resulting in surface overflow from the bioretention cell.

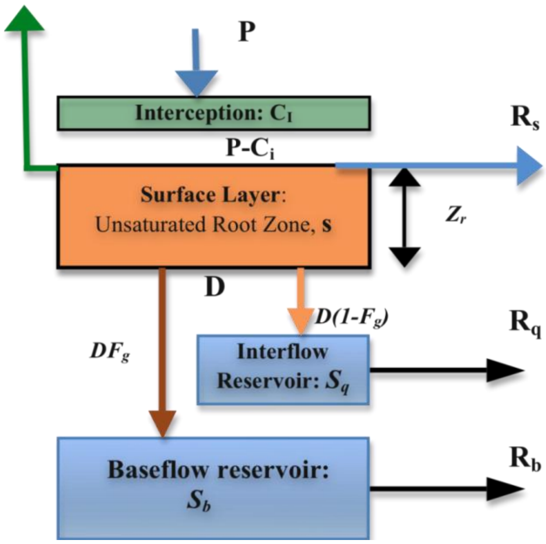

Figure 7. Bioretention Model

**$R_s$:** Direct surface runoff.
**$R_q$:** Throughflow, lateral flow, or quick flow.
**Zr:** root zone depth
**$R_b$:** base flow
**D:** Percolation, leakage, or drainage from the root zone
**Fg:** fraction of the leakage that goes to the groundwater reservoir

**BMP Treatment Train and Options**

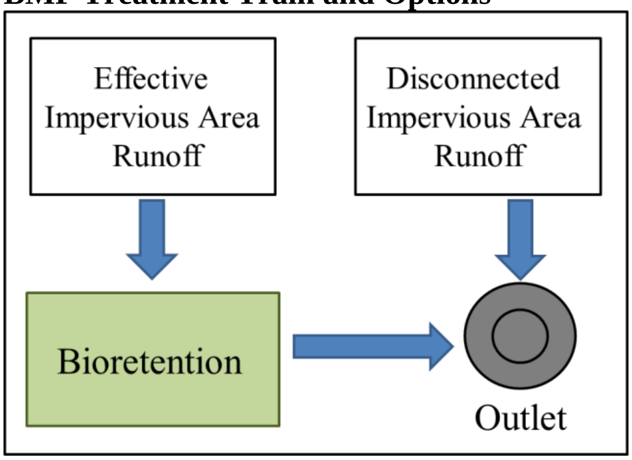

Figure 8. BMP Treatment Train

- 1 bio cell for every 1000 sqft of impervious surface
- Overflow is directly connected to stormdrain
- Collects runoff from rooftops, roads, driveways, and parking lots
- Bioretention cells collect water from EIA (20% of basin)
- 2,329 cells for total EIA treatment

| Bioretention dimensions | | |
|---|---|---|
| | Option 1 | Option 2 |
| length (ft) | 4.1 | 10 |
| width (ft) | 4.1 | 10 |
| weir height (ft) | 1 | 1 |
| soil depth (ft) | 2 | 2 |
| loamy sand porosity | 0.42 | 0.42 |
| area of footprint ($ft^2$) | 16.81 | 100 |
| volume of storage (gal) | 231.38 | 1376.42 |
| infiltration capacity (in/hr) | 1.34 | 1.34 |

Table 5. Bioretention cell options

# Results

### Water Balance Ratios

| Model Output | ETa/P | Q/P | Drainage/P |
|---|---|---|---|
| Forested | 0.503 | 0.065 | 0.431 |
| Urban, no BMP | 0.313 | 0.237 | 0.450 |
| Urban, BMP Option 1 | 0.311 | 0.201 | 0.448 |
| Urban, BMP Option 2 | 0.306 | 0.123 | 0.440 |

### Flow duration Curves

Forested condition and urban land use, no treatment

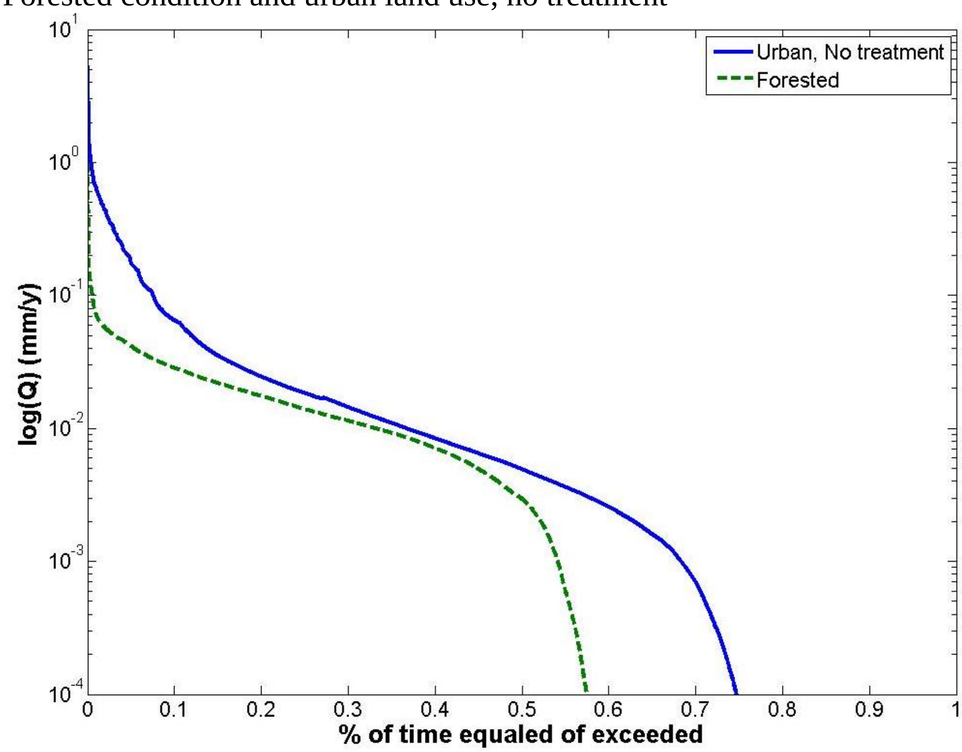

BMP Treatment Option 1

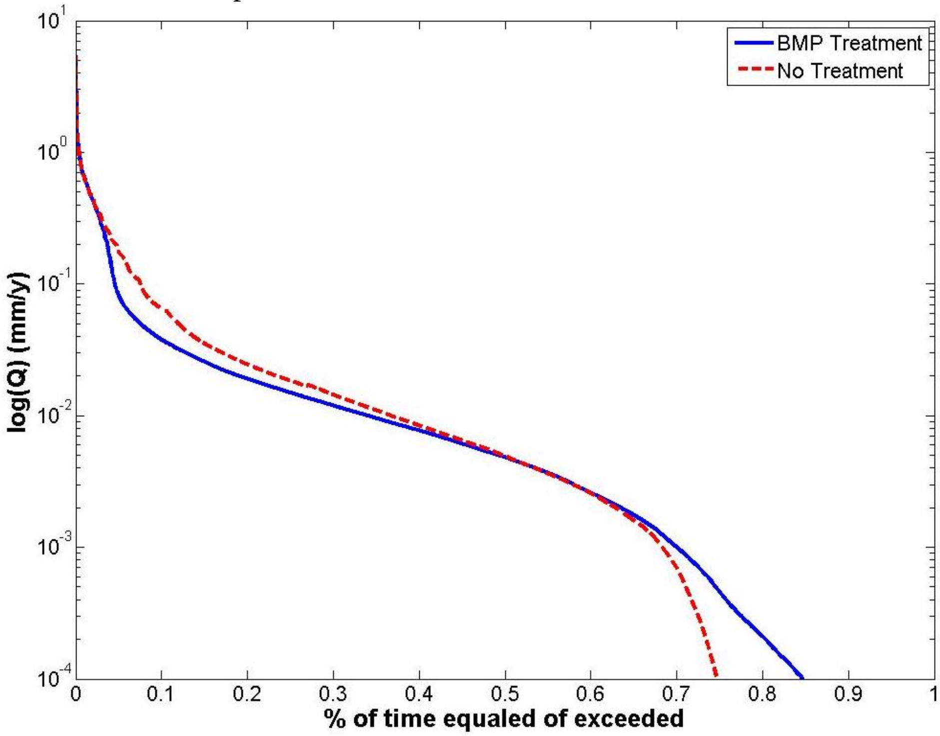


BMP Treatment Option 2

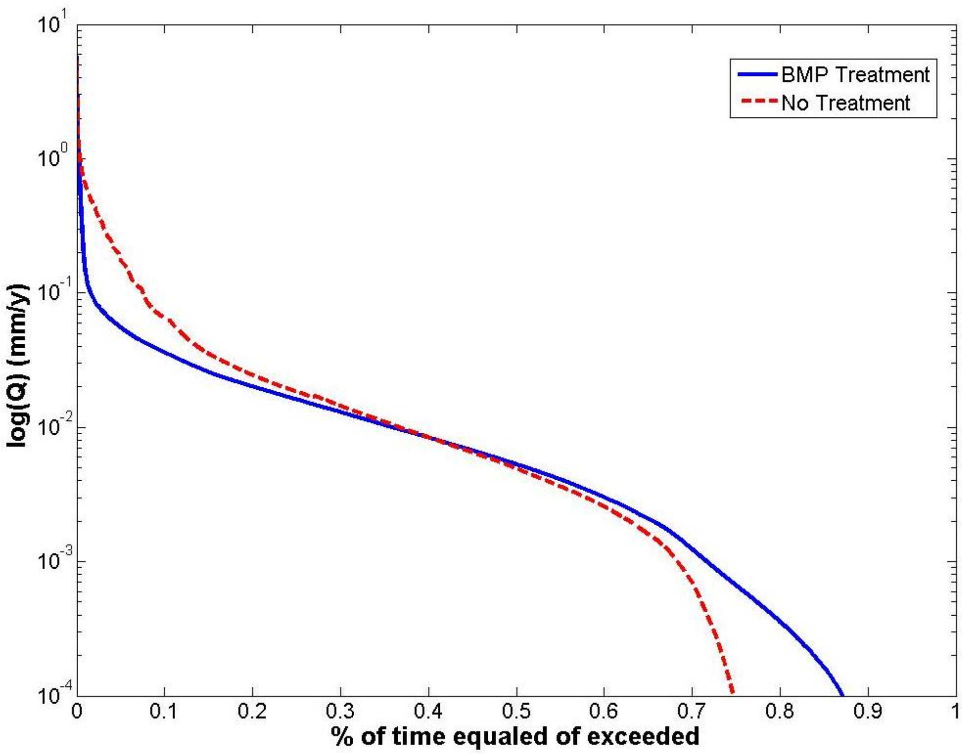

**Hydrologic indicators**

Indicator target ranges:

| B-IBI Goal | Stream Condition | HPC | HPR | PEAK:BASE |
|---|---|---|---|---|
| > 35 | Good | 3.0 – 7.0 | 90 – 110 | 6.7 – 28.3 |
| 30 – 35 | Fair | 2.0 – 8.7 | 34 – 168 | 6.7 – 28.8 |
| 24 – 29 | Poor | 7.3 – 10.7 | 115 – 178 | 3.5 – 45.0 |
| < 16 | Very Poor | 10.0 – 22.0 | 160 – 306 | 13.0 – 40.0 |

**Current Conditions**

| Indicator | Observed Conditions (3-yr calibration) | Long-term modeled Conditions (12-yrs) | B-IBI Stream Health |
|---|---|---|---|
| Mean HPC | 21.7 | 30.3 | Very Poor |
| Mean HPR | 268.3 | 341.6 | Very Poor |

**Forested Conditions**

| Indicator | Forested Conditions | B-IBI Stream Health |
|---|---|---|
| Mean HPC | 1.3 | Good |
| Mean HPR | 26.6 | Good |

BMP Treatment: Option 1

| Indicator | BMP Treatment (12-year) | B-IBI Stream Health |
|---|---|---|
| Mean HPC | 25.2 | Very Poor |
| Mean HPR | 323.6 | Very Poor |

BMP Treatment: Option 2

| Indicator | BMP Treatment | B-IBI Stream Health |
|---|---|---|
| Mean HPC | 9.4 | Poor |
| Mean HPR | 241.2 | Very Poor |

**Mean Annual Runoff Ratios for Puget Sound Basins**

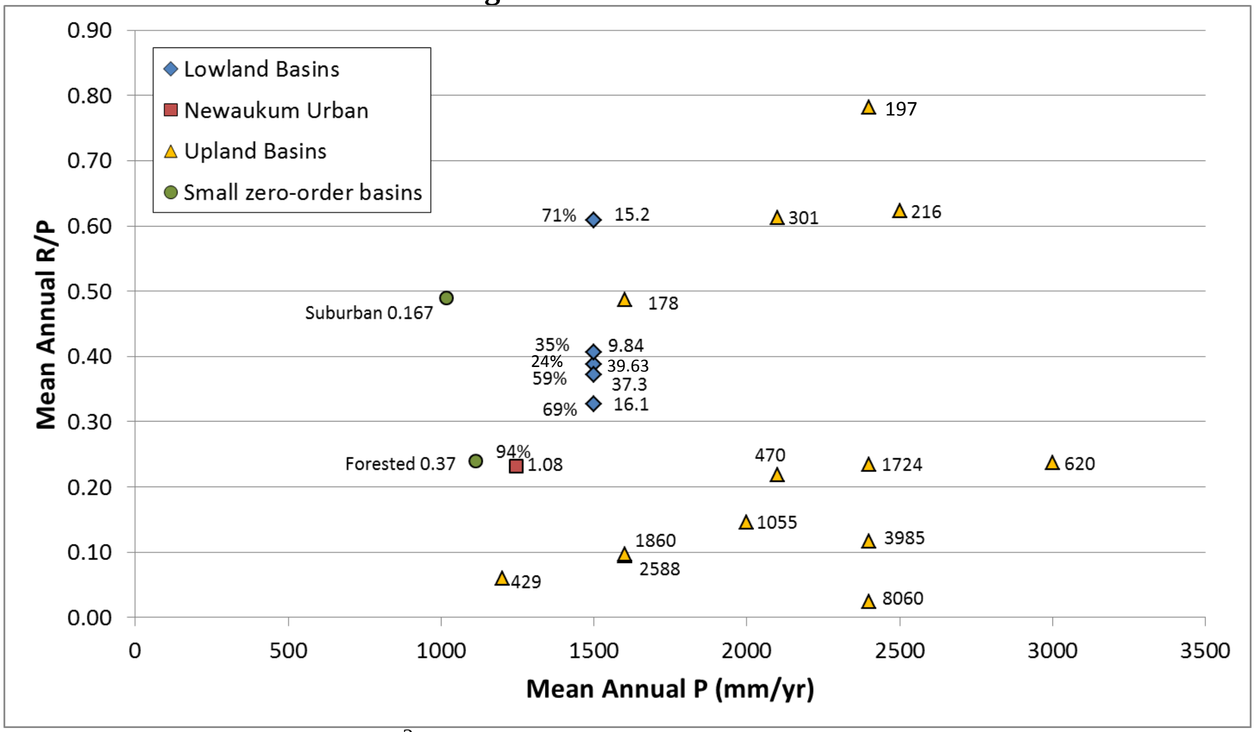


*Numbers are basin area in km$^2$
*Percentages are basin urbanization fraction
*Lowland and Upland basin data from Cuo et al. 2008
*Small zero-order basin data from Burges et al. 1998

**References**

ASCE-EWRI (2005). The ASCE Standardized Reference Evapotranspiration Equation. Report of the Task Committee on Standardization of Reference Evapotranspiration. Environmental and Water Resources Institute of the American Society of Civil Engineers, Reston, Virginia, USA.

DeGasperi et al. (2009). Linking hydrologic alteration to biological impairment in urbanization streams of the Puget Lowland, Washington, USA. *Journal of American Water Resource Association*, 45(2), 512-533.

Boyd, M.J., M. C. Bufill, R. M. Knee (1993). Pervious and impervious runoff in urban catchments, *Hydrological Sciences*, 38(6), 463-478.

Boyd, M.J., M. C. Bufill, R. M. Knee (1994). Predicting pervious and impervious storm runoff from urban drainage basins, *Hydrological Sciences*, 39(4), 321-332.

Burges, S.J., M.S. Wigmosta, and J.M. Meena (1998). Hydrological effects of land-use change in a zero-order catchment, *Journal of Hydrologic Engineering*, 3, 86-97.

Campbell, G. S. (1974). A simple method for determining unsaturated conductivity from moisture retention data, *Soil Sciences*, 117, 3311-314.

Chapman, T. (1991). Comment on ''Evaluation of automated techniques for base flow and recession analyses'' by R. J. Nathan and T. A. McMahon, *Water Resources Research*, 27, 1783–1784.

Cuo, L., D. P. Lettenmaier, B.V. Mattheussen, P. Storck, and M Wiley (2008). Hydrologic prediction for urban watersheds with the Distributed Hydrology-Soil-Vegetation Model, *Hydrologic Processes*, doi: 10.1002/hyp.7023.

Fore, L.S., J.R. Karr. And R.W. Wisseman (1996). Assessing Invertebrate Responses to Human Activities: Evaluating Alternative Approaches. *Journal of the North American Benthological Society* 15(2), 212-231.

Hino, M., and M. Hasabe (1984). Identification and prediction of nonlinear hydrologic systems by the filter-separation autoregressive (AR) method: extension to hourly hydrologic data, *Journal of Hydrology*, 68, 181-210.

Horner, R.R., D.B. Booth, A. Azous, and C.W. May (1997). Watershed Determinants of Ecosystem Functioning. In L.A. Roesner (ed.), Effects of Watershed Development and Management on Aquatic Ecosystems, *American Society of Civil Engineers*, New York, NY, 251-274.

Horner, R. (2011). Development of Flow and Water Quality Indicators. Unpublished Status Report.

Horner, R. (2012). Development of Flow and Water Quality Indicators. Unpublished Status Report.

Istanbulluoglu, E., T. Wang, and D. A. Wedin (2012). Evaluation of ecohydrologic model parsimony at local and regional scales in a semiarid grassland ecosystem, *Ecohydrology*, 5, 121-142.

Karr, J.R., and C.O. Yoder (2004). The Biological Assessment and Criteria Improve Total Maximum Daily Load Decision Making, *Journal of Environmental Engineering*, 130 (6), 594-604.

Laio, F., A. Porporato, L. Ridolfi, I Rodriguez-Iturbe (2001). Plants in water controlled ecosystems: Active role in hydrologic processes and response to water stress II. Probabilistic soil moisture dynamics, *Advances in Water Resources*, 24, 707-723.

Linsley, R. K., M.A. Kohler, and J.L.H. Paulhus (1958). Hydrology for Engineers, McGraw-Hill, New York.

May, C.W. (1996). Assessment of Cumulative Effects of Urbanization on Small Streams in the Puget Sound Lowland Ecoregion: Implications for Salmonid Resource Management. Ph.D. dissertation, University of Washington, Seattle, WA, U.S.A.

May, C.W., E.B. Welch, R.R. Horner, J.R. Karr, and B.W. Mar (1997). Quality Indices for Urbanization Effects in Puget Sound Lowland Streams. Washington Department of Ecology, Olympia, WA.

Nathan, R. J., and T. A. McMahon (1990). Evaluation of automated techniques for base flow and recession analyses, *Water Resources Research*, 26, 1465– 1473.

Smakhtin, V. U. (2001). Low flow hydrology: A review, *Journal of Hydrology.*, 240, 147– 186.

Shoemaker, L., J. Riverson Jr., K. Alvi, J. X. Zhen, S. Paul, and T. Rafi (2009). SUSTAIN - A Framework for Placement of Best Management Practices in Urban Watersheds to Protect Water Quality. EPA/600/R-09/095. U.S. Environmental Protection Agency, Water Supply and Water Resources Division, National Risk Management Research Laboratory, Cincinnati, OH.

Sujono, J., S. Shikasho, and K. Hiramatsu (2004). A comparison of techniques for hydrograph recession analysis, *Hydrological Processes*, 18, 403-313.

Wang, T., E. Istanbulluoglu, J. Lenters, and D. Scott (2009). On the role of groundwater and soil texture in the regional water balance: An investigation of the Nebraska Sand Hills, USA, *Water Resources Res*earch, 45, W10413, doi:10.1029/2009WR007733.